Check for updates

KNOX Protein OSH15 Induces Grain Shattering by Repressing Lignin Biosynthesis Genes[1][OPEN]

Jinmi Yoon[2], Lae-Hyeon Cho[2], Htet Wai Antt, Hee-Jong Koh, and Gynheung An*

Crop Biotech Institute and Graduate School of Biotechnology, Kyung Hee University, Yongin 446-701, Korea (J.Y., L.-H.C., H.W.A., G.A.); and Department of Plant Science, Research Institute of Agriculture and Life Sciences, and Plant Genomics and Breeding Institute, Seoul National University, Seoul 151-921, Korea (H.-J.K.)

ORCID ID: 0000-0002-8570-7587 (G.A.).

Seed shattering is an agronomically important trait. Two major domestication factors are responsible for this: qSH1 and SH5. Whereas qSH1 functions in cell differentiation in the abscission zone (AZ), a major role of SH5 is the repression of lignin deposition. We have determined that a KNOX protein, OSH15, also controls seed shattering. Knockdown mutations of *OSH15* showed reduced seed-shattering phenotypes. Coimmunoprecipitation experiments revealed that OSH15 interacts with SH5 and qSH1, two proteins in the BELL homeobox family. In transgenic plants carrying the *OSH15* promoter-*GUS* reporter construct, the reporter gene was preferentially expressed in the AZ during young spikelet development. The RNA in situ hybridization experiment also showed that *OSH15* messenger RNAs were abundant in the AZ during spikelet development. Analyses of *osh15 SH5*-D double mutants showed that *SH5* could not increase the degree of seed shattering when *OSH15* was absent, indicating that SH5 functions together with OSH15. In addition to the seed-shattering phenotype, *osh15* mutants displayed dwarfism and accumulated a higher amount of lignin in internodes due to increased expression of the genes involved in lignin biosynthesis. Knockout mutations of *CAD2*, which encodes an enzyme for the last step in the monolignol biosynthesis pathway, caused an easy seed-shattering phenotype by reducing lignin deposition in the AZ. This indicated that the lignin level is an important determinant of seed shattering in rice (*Oryza sativa*). Chromatin immunoprecipitation assays demonstrated that both OSH15 and SH5 interact directly with *CAD2* chromatin. We conclude that OSH15 and SH5 form a dimer that enhances seed shattering by directly inhibiting lignin biosynthesis genes.

During crop domestication, one challenge is controlling the degree of grain shattering (Fuller and Allaby, 2009). While easy shattering causes a loss of seeds before harvest, nonshattering leads to difficulties when that grain is being threshed (Ji et al., 2010). Seed dispersal is affected by the development of the abscission zone (AZ) and lignification (Lewis et al., 2006; Estornell et al., 2013; Dong et al., 2014; Dong and Wang, 2015). Differentiated AZ cells are smaller and isodiametrically compacted when compared with the surrounding cells (Zhou et al., 2012). In rice (*Oryza sativa*), the AZ develops between the sterile lemma and rudimentary glume when panicles are 5 to 30 mm long (Ji et al., 2010).

The major quantitative trait locus for seed shattering in rice, *qSH1*, encodes a BELL homeobox protein. A single-nucleotide polymorphism in its 5′ regulatory region can block its expression, resulting in defective AZ development (Konishi et al., 2006). Another BELL homeobox gene, *SH5*, which is highly homologous to *qSH1*, also controls seed shattering mainly in *indica* cultivars (Yoon et al., 2014). Expression of the former is detected in young spikelets, especially within the AZ, lamina joint, and intercalary meristem (IM) region. *SH5* induces two transcription factor genes, *SHAT1* and *Sh4*, that are essential for appropriate AZ development (Li et al., 2006; Zhou et al., 2012; Yoon et al., 2014). Although *SH5* is unable to induce the formation of a proper AZ, the gene causes grain shattering by repressing lignin deposition in the pedicel region (Yoon et al., 2014).

BELL and KNOX proteins are three-amino acid-loop-extension (TALE) superclass transcription factors; the tandem complex of BELL and KNOX regulates the expression of target genes in developmental processes (Chen et al., 2003; Kanrar et al., 2006; Hay and Tsiantis,

[1] This work was supported by the Cooperative Research Program for Agriculture Science and Technology Development, Rural Development Administration, Republic of Korea (grant no. PJ01108001), and by the Republic of Korea Basic Research Promotion Fund (grant no. NRF-2007-0093862).

[2] These authors contributed equally to the article.

* Address correspondence to genean@khu.ac.kr.

The author responsible for distribution of materials integral to the findings presented in this article in accordance with the policy described in the Instructions for Authors (www.plantphysiol.org) is: Gynheung An (genean@khu.ac.kr).

G.A. organized the entirety of this research; G.A., J.Y., L.-H.C., and H.-J.K. designed the research; J.Y., L.-H.C., and H.W.A performed the experiments; J.Y., L.-H.C., and G.A. wrote the article.

[OPEN] Articles can be viewed without a subscription.

www.plantphysiol.org/cgi/doi/10.1104/pp.17.00298

 © 2017 American Society of Plant Biologists. All Rights Reserved.

2010). Interactions between BELL and KNOX proteins have been observed in barley (*Hordeum vulgare*; Müller et al., 2001), Arabidopsis (*Arabidopsis thaliana*; Smith and Hake, 2003), maize (*Zea mays*; Smith et al., 2002), and potato (*Solanum tuberosum*; Chen et al., 2003). In potato, the complex of StBEL5 and POTATO HOMEOBOX1 is required to repress the expression of *GA20OX1* by directly binding to the specific (T/A)GA (C/G)(T/A)(T/A)GAC site in the promoter region (Chen et al., 2003).

Arabidopsis BREVIPEDICELLUS (BP), encoding a KNOX protein, suppresses the transcription of the lignin biosynthesis genes PHENYLALANINE AMMONIA LYASE1 (PAL1), cinnamic acid 4-hydroxylase, 4-coumarate-coenzyme A ligase, cinnamyl alcohol dehydrase 1, caffeic acid *O*-methyltransferase (COMT), and caffeoyl coenzyme A 3-*O*-metyltransferase (CCoAoMT) by directly binding in the COMT and CCoAoMT promoter regions (Mele et al., 2003). The *bp* null mutant causes pleiotropic phenotypes such as short internodes, downward-facing siliques, and irregular epidermis cells (Venglat et al., 2002).

The rice genome has five functional class I KNOX genes: *OSH1*, *OSH6*, *OSH15*, *OSH43*, and *OSH71* (Tsuda et al., 2011). They are preferentially expressed in the indeterminate cells around the shoot apical meristem (SAM) and are necessary for the formation and maintenance of that SAM (Hake et al., 2004; Tsuda et al., 2011; Luo et al., 2012). The *osh1* null mutant has a defect in the SAM and shows arrested development at the three-leaf stage (Sato et al., 1996; Tsuda et al., 2011). A loss-of-function mutation in *OSH15* exhibits a dwarf phenotype that results from defective internodal elongation of the uppermost region (Sato et al., 1999).

In this study, we determined that OSH15 functions in seed shattering by binding to SH5 and qSH1, two major domestication factors for seed shattering, by directly inhibiting lignin biosynthesis genes.

RESULTS

Knockdown Mutations in *OSH15* Reduce Seed Shattering

We isolated rice line 1D-03912, in which the T-DNA is inserted 380 bp upstream from the ATG start codon of *OSH15* (Fig. 1A). The expression of *OSH15* was decreased significantly in the *osh15-1* mutant (Fig. 1B). The knockdown mutant showed a reduced seed-shattering phenotype. Values calculated for the breaking tensile strength (BTS) of the pedicel, which represents nonshattering degree, were significantly higher in the mutant than in the segregating cv Dongjin wild type, which had a moderate shattering phenotype (Fig. 1C). To study whether the mutant phenotype is due to a defect in AZ development, we examined longitudinal sections of mature spikelets at the heading stage. Whereas the AZ was well developed in the wild-type spikelets (Fig. 1, D and F), it was significantly retarded in the mutant (Fig. 1, E and G).

To confirm that the mutant phenotype was due to a defect in *OSH15*, we generated transgenic plants expressing *OSH15* RNA interference (RNAi) in the *indica* cv Kasalath, which shows an easy-shattering phenotype. The 3′ untranslated region (UTR) of *OSH15* was used to produce the transgenics (Fig. 2A). When compared with the wild type, endogenous *OSH15* expression declined to very low levels in the RNAi transgenic plants (Fig. 2B). All transgenic plants displayed a reduced seed-shattering phenotype when compared with the parental and segregating wild-type plants. Values for BTS were increased significantly

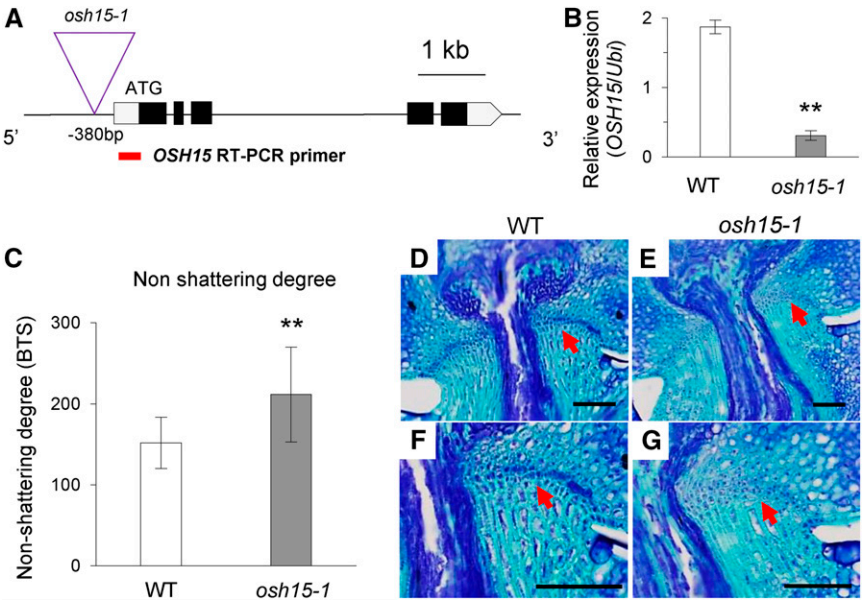

Figure 1. Identification and characterization of the *osh15-1* mutant. A, Schematic diagram of *OSH15* genome structure and T-DNA insertion line 1D-03912. Boxes indicate exons; lines between boxes are introns. T-DNA was inserted 380 bp upstream from the start ATG. The red line indicates the reverse transcription (RT)-PCR product for the expression analysis of *OSH15*. B, Transcript levels of *OSH15* in the wild type (WT) and the *osh15*-1 mutant. RNA samples were collected from second internodes immediately before heading stage ($n = 4$; **, $P < 0.01$). C, Degree of shattering in segregated wild-type and *osh15-1* mutant plants ($n = 10$ or more; **, $P < 0.01$). D to G, Longitudinal sections across the AZ from the wild type (D and F) and the *osh15-1* mutant (E and G) immediately before heading stage. Samples were stained with Toluidine Blue. Arrows indicate AZ. Bars = 200 μm.

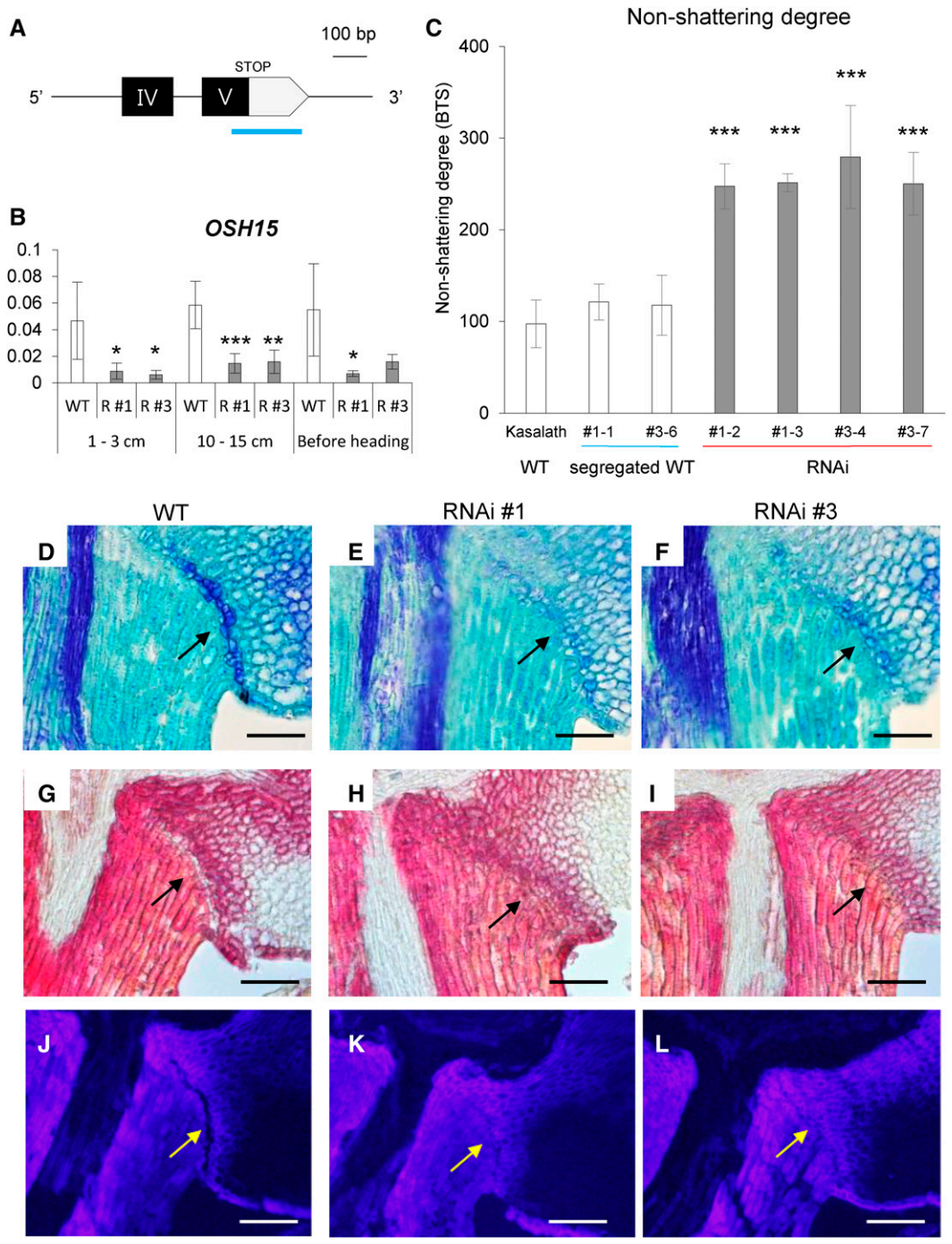

Figure 2. Analysis of *OSH15* RNAi transgenic plants in cv Kasalath. A, Schematic diagram of the *OSH15* RNAi region. The 265-bp 3′ UTR (blue line) fragment was used to generate the *OSH15* RNAi construct. B, Expression levels of *OSH15* in transgenic plants. Developing panicles were used ($n = 4$; *, $P < 0.05$; **, $P < 0.01$; and ***, $P < 0.001$). C, Degree of shattering in the cv Kasalath segregated wild type and *OSH15* RNAi lines ($n = 10$ or more; ***, $P < 0.001$). D to I, Longitudinal sections across the AZ before harvest from the cv Kasalath wild type (WT; D and G) and RNAi lines 1 (E and H) and 3 (F and I). Sections were stained with Toluidine Blue (D–F) or phloroglucinol-HCl (G–I). Arrows indicate AZ. Bars = 100 μm. J to L, Longitudinal sections across the AZ after heading from the cv Kasalath wild type (J), RNAi line 1 (K), and RNAi 3 (L). Sections were observed under UV light. Arrows indicate AZ. Bars = 100 μm.

in the *OSH15* RNAi transgenic plants (Fig. 2C). Longitudinal sections of mature spikelets revealed that AZ development was diminished significantly in the RNAi plants (Fig. 2, D–L). These observations confirmed that *OSH15* modulates the degree of seed shattering.

Expression Pattern of *OSH15*

RNA in situ hybridization demonstrated that *OSH15* is expressed just below the leaf insertion regions and at the primordia of axillary buds (Sato et al., 1999). To study those patterns at the tissue level, we generated transgenic rice plants that express the *GUS* reporter gene under the control of the 1.7-kb *OSH15* promoter region (Fig. 3A).

We performed quantitative reverse transcription (qRT)-PCR analysis and GUS assays with various tissues to investigate whether mRNA levels of *OSH15* coincide with GUS expression patterns (Supplemental Fig. S1). At the seedling stage, *OSH15* mRNA levels were low in leaves but relatively higher in SAM regions and roots. GUS staining produced similar results, with marker expression being barely detectable in leaf vascular tissues but strong in the SAM and roots. At the mature stage, transcript levels of *OSH15* were much higher in the stems, young panicles, and mature spikelets. Similar results were obtained with GUS staining. This suggested that the pattern of endogenous *OSH15* expression is correlated with that of GUS expression when driven by the 1.7-kb *OSH15* promoter.

The AZ forms between the sterile lemma and rudimentary glume at spikelet development stage Sp7, when panicles are 5 to 30 mm long (Itoh et al., 2005; Ji et al., 2010). Our analyses of *GUS* patterns in the young spikelets from transgenic plants showed that *OSH15* was expressed preferentially in the AZ zone during Sp7 (Fig. 3C) and early in Sp8 (Fig. 3D). In mature spikelets, the reporter gene was expressed mainly in the pedicel and spikelet junction region (Fig. 3E). The RNA in situ

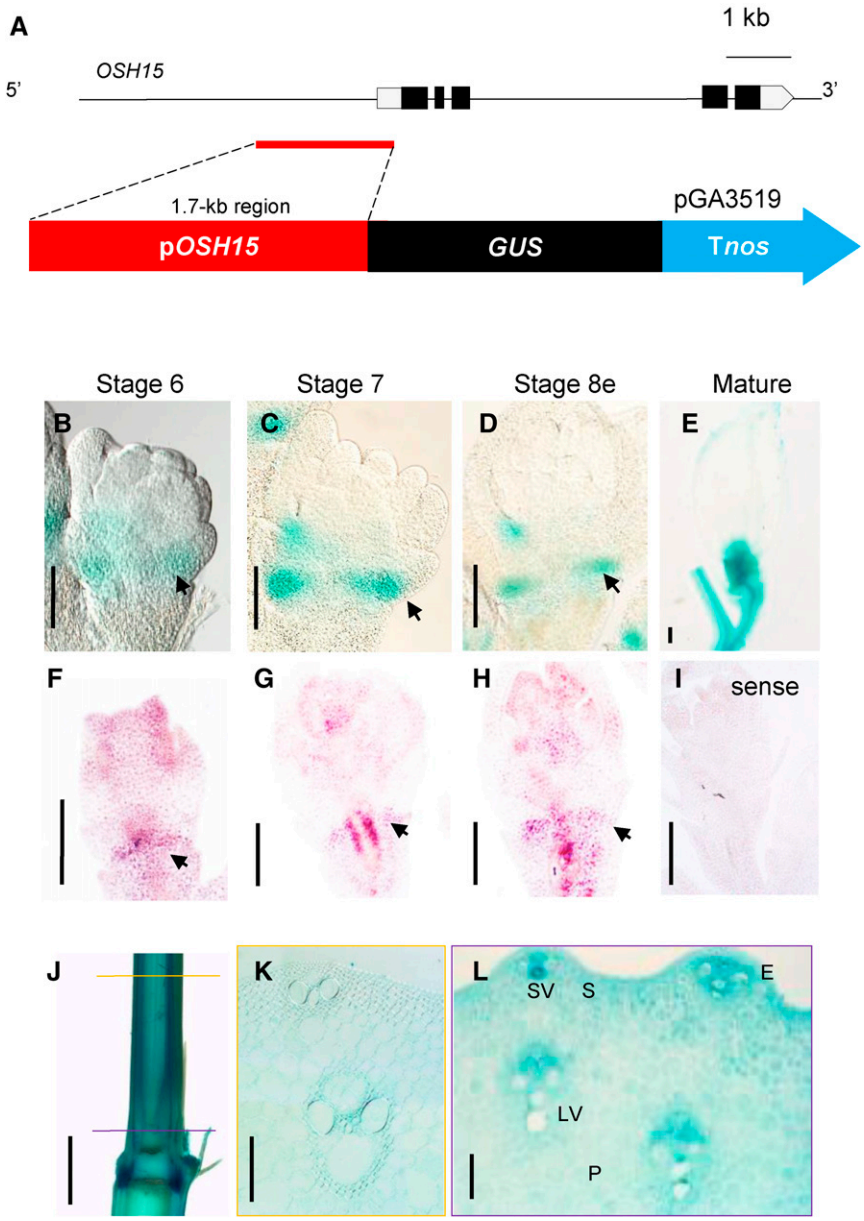

Figure 3. Expression patterns of *OSH15* at the AZ and internode. A, Schematic diagram of the *OSH15* pro::GUS construct. B to E, GUS expression patterns at the AZ. Arrows indicate AZ. Bars = 200 μm. F to I, RNA in situ hybridization of *OSH15*. Arrows indicate AZ. Bars = 200 μm. J, Expression pattern of GUS in stems. The yellow line in the elongated region and the purple line in the meristem region indicate the positioning of cross sections. Bar = 2 mm. K and L, Cross sections of the elongated region (K) and the meristem region (L) at the indicated positions in F. E, Epidermis; LV, large vein; P, parenchyma cell; S, sclerenchyma cell; SV, small vein. Bars = 100 μm.

hybridization experiment also showed that *OSH15* mRNAs were abundant in the AZ during spikelet development (Fig. 3, F–I). The *GUS* reporter also was expressed in the stems (Fig. 3J). Cross sections of the elongation zone and meristem region showed that *OSH15* was expressed ubiquitously, albeit more prominently in vascular tissues (Fig. 3, K and L).

OSH15 Interacts with BELL-Type Homeobox Proteins

Class I KNOX proteins bind to BELL proteins through the conserved MEINOX domain of the former and the MEINOX-interacting domain (MID) of the latter (Supplemental Fig. S2A; Chen et al., 2003). This TALE-HD complex regulates downstream genes by repressing transcriptional activation (Chen et al., 2003). Both Arabidopsis and rice encode nine class I KNOX proteins each (Supplemental Fig. S2B). For the BELL family, 13 members are present in Arabidopsis and 17 members are present in rice (Supplemental Fig. S2C).

Two major domestication factors for seed shattering, SH5 and qSH1, belong to the BELL family (Konishi et al., 2006; Yoon et al., 2014). We performed coimmunoprecipitation (Co-IP) experiments to investigate

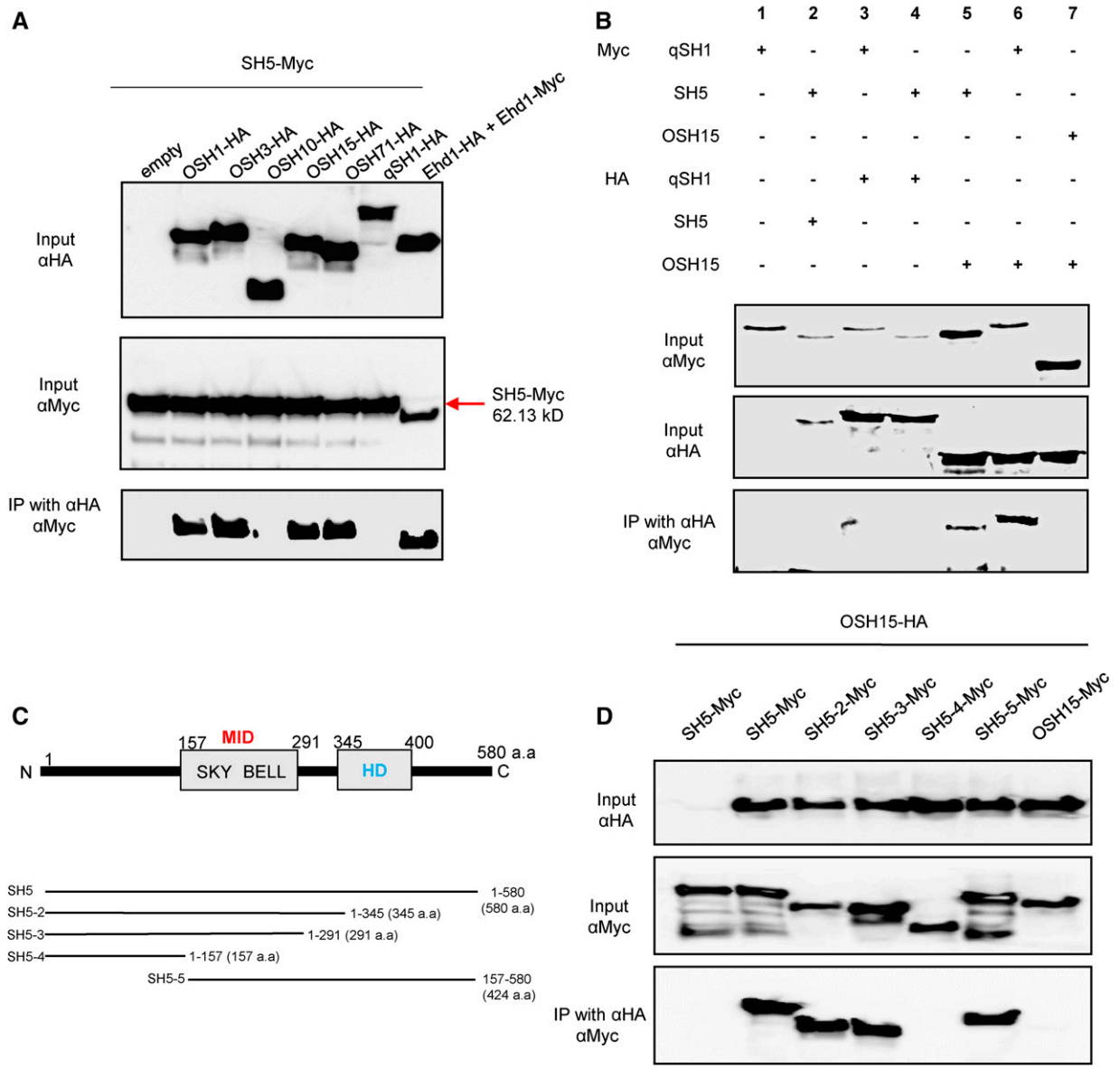

Figure 4. Interaction analyses by Co-IP assays. A, Analysis of heterodimerization between KNOX proteins and SH5. Assays were performed using SH5 tagged with Myc and the KNOX proteins OSH1, OSH3, OSH10, OSH15, and OSH71 tagged with HA. B, Analysis of heterodimerization between SH5 and OSH15 and between qSH1 and OSH15. C, Schematic diagrams of SH5 and truncated forms. a.a., Amino acids; BELL, BEL-like; HD, homeodomain; SKY, Ser, Lys, and Tyr residues. D, Co-IP assay of OSH15 and SH5 truncated forms.

whether OSH15 interacts with SH5. The full-length cDNA of OSH15 was fused to the HA tag and SH5 was fused to the Myc tag. The fusion proteins were coexpressed in protoplasts isolated from rice callus suspension cells. After immunoprecipitation by anti-HA antibodies, protein interactions were detected with anti-Myc antibodies. The results of this experiment confirmed that OSH15 interacts with SH5 (Fig. 4A). Examination of four additional class I KNOX proteins showed that OSH1, OSH3, and OSH71 also bind to SH5 but OSH10 does not (Fig. 4A). Instead, OSH10 possesses only a partial sequence of the MEINOX domain, which implies that a complete MEINOX domain is needed for such interactions. OSH15 also binds to qSH1, which is highly homologous to SH5 (Fig. 4B, sample 6). Homodimerization tests of qSH1, SH5, and OSH15 showed that they do not form a homodimer (Fig. 4B, samples 2, 3, and 7).

To determine which domain is responsible for the interaction, we generated constructs for truncated forms of SH5 (Fig. 4C). Deletion of the HD domain did not interfere with its ability to bind to OSH15 (Fig. 4D, lanes 2 and 3). However, further deletion of the MID, which contains SKY and BELL regions, resulted in a loss of binding (Fig. 4D, lane 4). Thus, we concluded that the MID is indeed necessary for this interaction between SH5 and OSH15.

We reported previously that *SH5* increases the degree of seed shattering when overexpressed in an activation tagging line (Yoon et al., 2014). Here, we introduced the activated *SH5* into the *osh15-1* mutant by crossing the two lines. This homozygous double mutant displayed the same shattering habit as *osh15-1* (Fig. 5). Therefore, this genetic analysis supported our theory that SH5 cannot function alone but requires OSH15 to induce seed shattering.

Expression of *Sh4*, a shattering transcription factor gene downstream of *SH5*, was examined in the pedicel region of *OSH15* RNAi transgenic plants while the AZ was developing there. Our qRT-PCR analyses confirmed that *OSH15* expression was reduced significantly in the RNAi plants (Supplemental Fig. S3A). However, transcript levels of *qSH1* and *SH5* were not altered, demonstrating that these BELL family genes were not affected by the mutation in the KNOX gene (Supplemental Fig. S3, B and C). In contrast, the expression of *Sh4* was downregulated significantly in the RNAi lines (Supplemental Fig. S3D).

Lignin Deposition Is Increased in the *osh15-1* Mutant

Seed shattering is induced when *SH5* represses lignin deposition at the AZ (Yoon et al., 2014). To determine whether *OSH15* also inhibits this deposition, we studied various expression patterns. In young panicles (0.5–3 cm long), most lignin biosynthesis genes were not expressed (Fig. 6). At a later stage, when panicles were 10 to 15 cm long, those genes in the wild type were expressed at higher levels in the junction region between the spikelet and the pedicel. Furthermore, the expression of *PAL1* was increased significantly in *OSH15* RNAi plants (Fig. 6A). Immediately before heading, the expression of *CAD2* was increased significantly in the transgenic plants (Fig. 6E). All of these results suggested that *OSH15* represses lignin biosynthesis in developing panicles.

In addition to having a seed-shattering phenotype, our knockdown mutants showed a dwarf phenotype (Fig. 7A), similar to a previous description of the *osh15* null mutant (Sato et al., 1999). The latter phenotype was caused by reduced internode elongation (Fig. 7, B and C). Lignin staining of cross sections from the second internode prior to harvest revealed that the *osh15-1* mutants accumulated more lignin when compared with the wild type. Those depositions occurred in the epidermal cells as well as in the sclerenchyma of vascular tissues in the wild type (Fig. 7, D and F). Samples from the mutant displayed increased amounts of lignin in the epidermal and sclerenchyma cells as well as ectopic lignin depositions between the small vascular tissues (Fig. 7, E and G). Increased lignin accumulations in the mutants also were observed before heading began (Fig. 7, I and K).

The expression of lignin biosynthesis genes was elucidated in the wild type and the *osh15-1* mutant

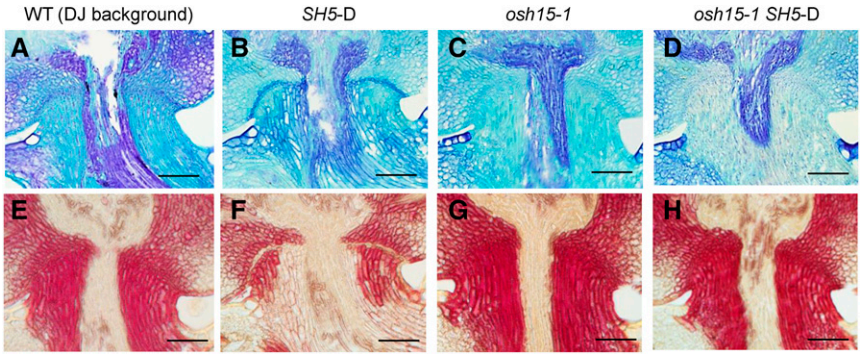

Figure 5. Analysis of the *osh15-1 SH5*-D double mutant. A to D, Preharvest AZ development shown via Toluidine Blue staining. A, The wild type (WT). B, *SH5*-D. C, *osh15-1*. D, The *osh15-1 SH5*-D double mutant. E to H, Preharvest lignin deposition shown via phloroglucinol-HCl staining. E, The wild type. F, *SH5*-D. G, *osh15-1*. H, The *osh15-1 SH5*-D double mutant. DJ, cv Dongjin. Bars = 200 μm.

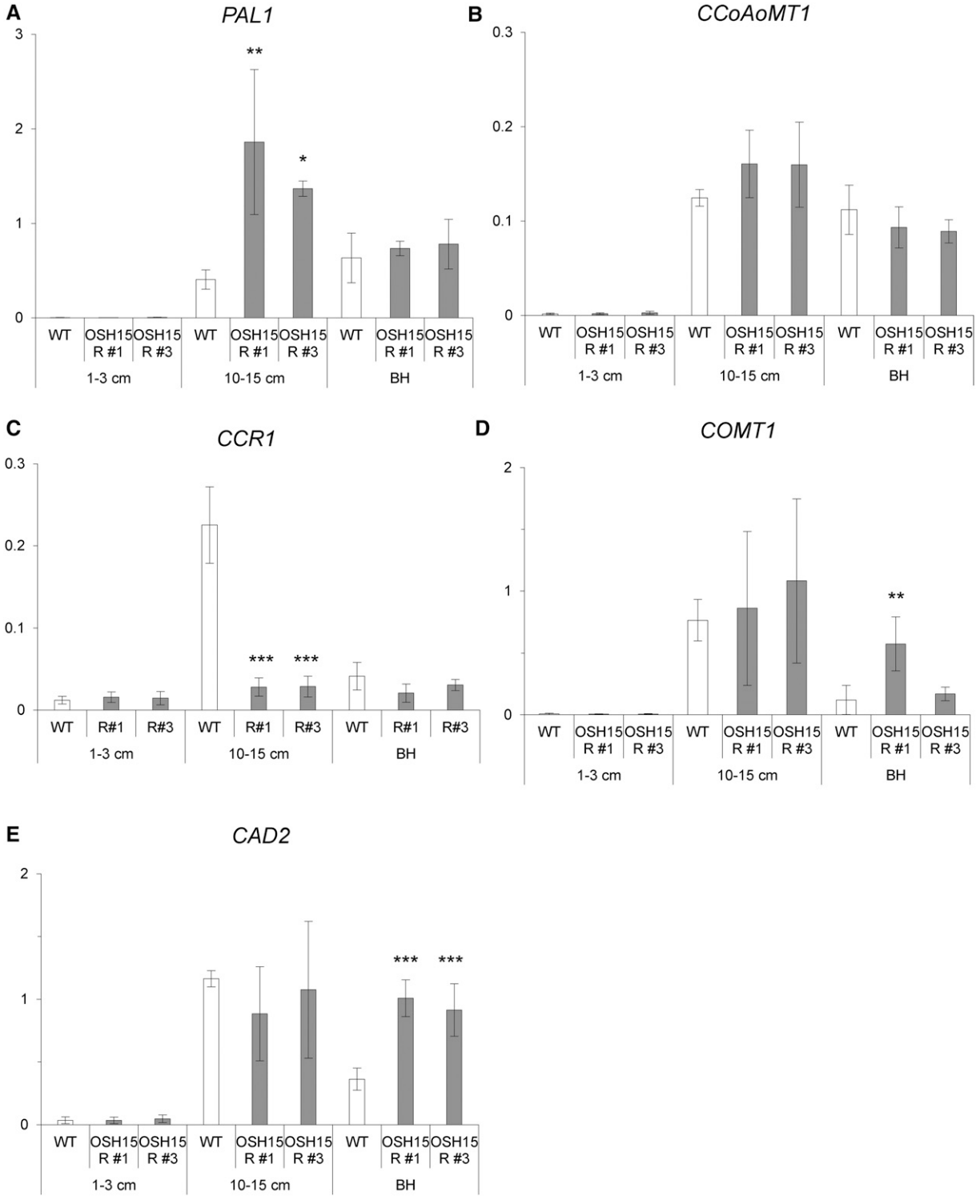

Figure 6. Expression levels of lignin biosynthesis genes during panicle development. The expression of *PAL1* (A), *CCoAoMT1* (B), *COMT1* (C), *CCR1* (D), and *CAD2* (E) was analyzed by qRT-PCR. The cv Kasalath wild type (WT) and *OSH15* RNAi lines 1 and 3 were examined at three developmental stages. Whole panicles were sampled when 1 to 3 cm long. Junction regions between panicles and the spikelet were sampled when panicles were 10 to 15 cm long and immediately prior to the heading stage ($n = 4$; *, $P < 0.05$; **, $P < 0.01$; and ***, $P < 0.001$). BH, Before heading.

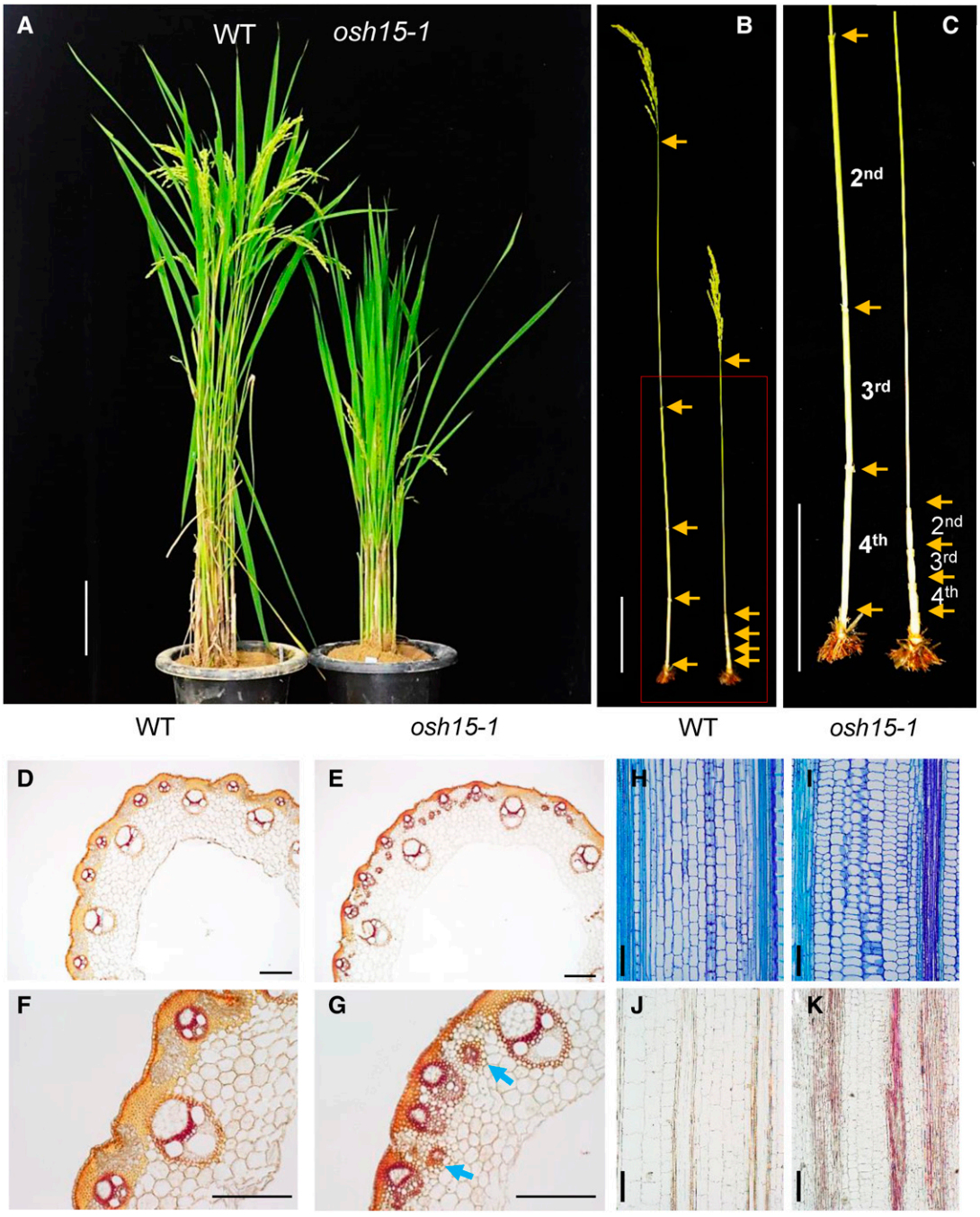

Figure 7. Phenotypes of the *osh15-1* mutant at the mature stage. A, Dwarfing phenotype of the *osh15-1* mutant compared with the segregated wild type (WT). Bar = 10 cm. B and C, Phenotypes of internodes from the wild type (left) and the *osh15-1* mutant (right). Arrows indicate nodes. Bars = 10 cm. D to G, Cross sections of the elongated region in the second internode before harvest in the wild type (D and F) and *osh15-1* (E and G). Samples were stained by phloroglucinol-HCl to observe lignin accumulations. Arrows indicate ectopic deposition. Bars = 200 μm. H to K, Longitudinal sections of the second internode immediately before heading in the wild type (H and J) and *osh15-1* (I and K). Samples were stained by Toluidine Blue (H and I) or phloroglucinol-HCl (J and K). Bars = 100 μm.

using internode samples collected from IM when the wild-type internodes were approximately 3 cm long. qRT-PCR analyses showed that transcript levels for *PAL1*, *COMT1*, *CCR1*, and *CAD2* were increased in the mutant (Fig. 8, C–G). The *OSH15* RNAi plants also presented semidwarf phenotypes and higher expression levels of the lignin biosynthesis genes, although these effects were less significant when

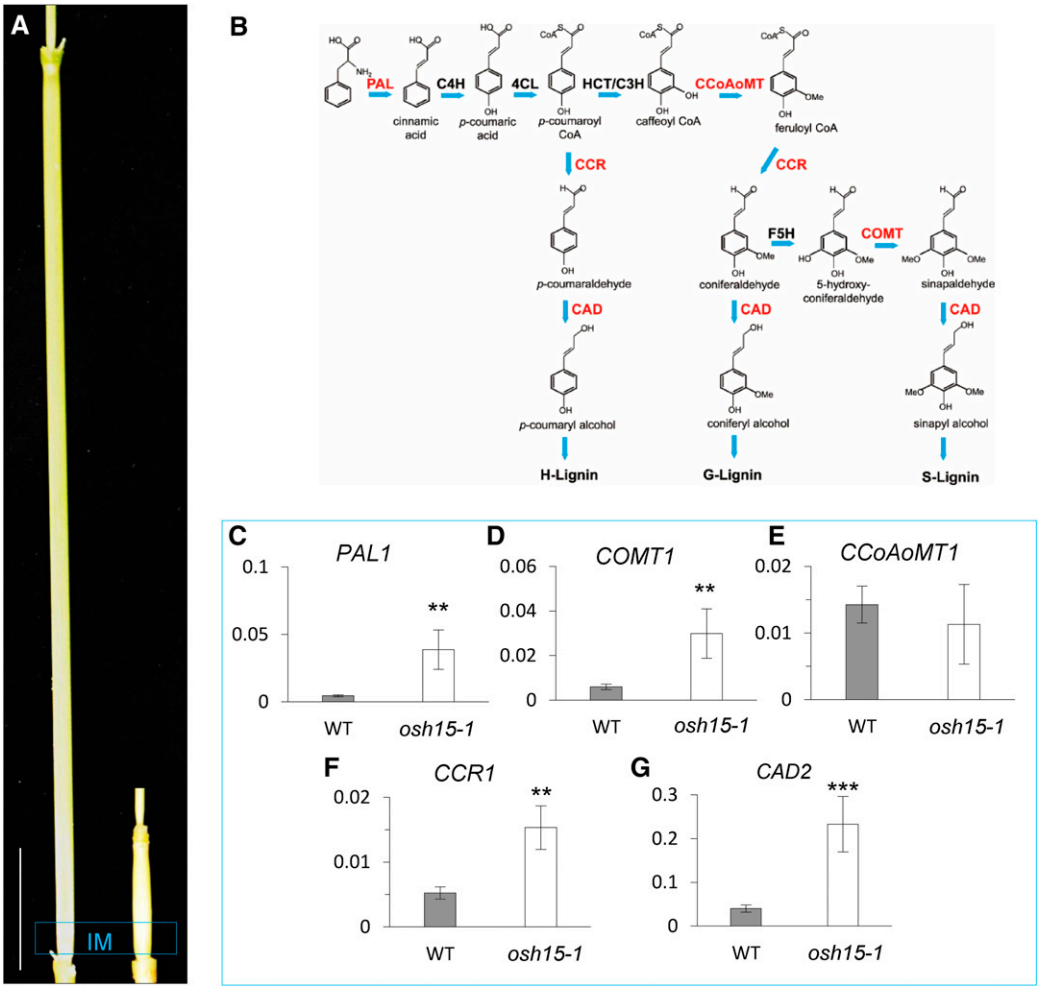

Figure 8. Expression patterns for lignin biosynthesis genes. A, Second internodes from the wild type (left) and the *osh15-1* mutant (right). The blue box indicates the IM region. Bar = 3 cm. B, Lignin biosynthesis pathway. PAL, Phe ammonia lyase; C4H, cinnamic acid 4-hydroxylase; 4CL, 4-coumarate-coenzyme A ligase; C3H, coumarate 3-hydroxylase; CCoAoMT, caffeoyl coenzyme A 3-*O*-metyltransferase; CCR, cinnamoyl-CoA reductase; F5H, ferulate 5-hydroxylase; COMT, caffeic acid *O*-methyltransferase; CAD, cinnamyl alcohol dehydrase. The genes examined by qRT-PCR are indicated in red. C to G, Expression patterns for *PAL1* (C), *COMT1* (D), *CCoAoMT1* (E), *CCR1* (F), and *CAD2* (G) in IM when wild-type (WT) internodes were approximately 3 cm long ($n = 4$; **, $P < 0.01$ and ***, $P < 0.001$).

compared with the *osh15-1* mutant (Supplemental Fig. S4).

Effects of Lignin Deposition on Seed Shattering and Internode Elongation

Within the lignin biosynthesis pathway, CAD functions in the last step of monolignol biosynthesis, catalyzing hydroxyl-cinnamyl aldehydes into their corresponding alcohols (Hirano et al., 2012). The relative ratios of these cinnamyl alcohols are essential for determining the structural and mechanical characters of lignin (Li et al., 2009). The rice genome has 12 CAD-like genes. Among them, the proteins encoded by *CAD2* and *CAD7* contribute to this enzyme activity, with *CAD2* being the most highly expressed (Hirano et al., 2012).

To extend our examination of the effect that lignin has on seed shattering, we isolated two independent T-DNA insertion lines in *CAD2*: 3A-01943 and 2B-50053 (Fig. 9A). Expression of this gene was completely abolished in each line, indicating that both contain null alleles (Fig. 9B). Calculations of BTS showed that both mutants display an easy-shattering phenotype (Fig. 9C). Toluidine Blue staining of the AZ in developing panicles revealed that AZ development was reduced significantly in the *cad2* mutants (Fig. 9, D–F). Visualization of lignin polymer level by a characteristic blue color under UV light revealed that lignin deposition was reduced significantly in the AZ as well as in the pedicles of the mutants (Fig. 9, G–I). These observations

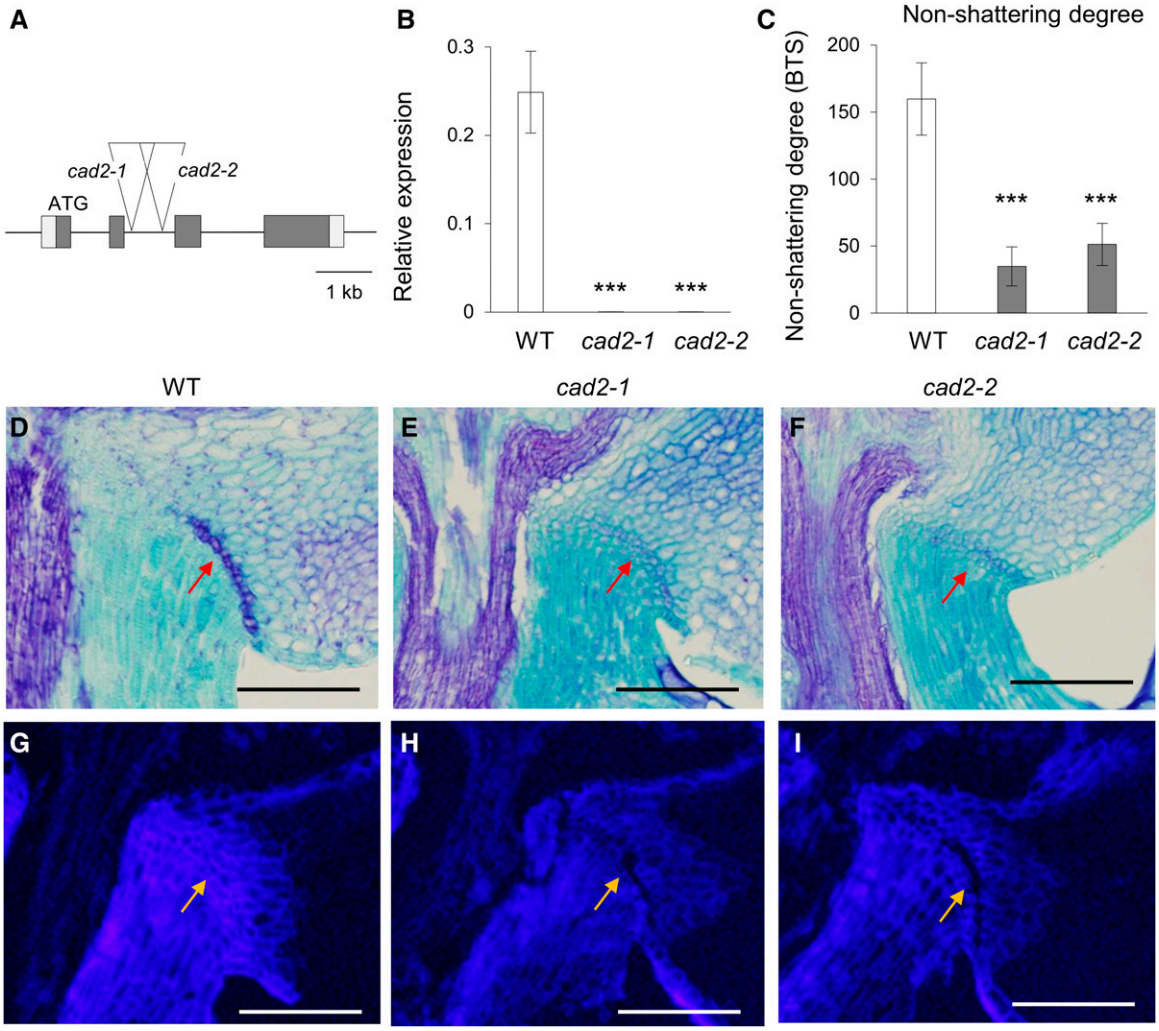

Figure 9. Phenotypes of *cad2* null mutants. A, Schematic diagram of the *CAD2* genome structure and T-DNA insertion positions in lines 3A-01943 (*cad2-1*) and 2B-50053 (*cad2-2*). Boxes indicate exons; lines between boxes are introns. Triangles located at the second intron indicate T-DNA. B, Transcript levels of *CAD2* in the wild type (WT), *cad2-1*, and *cad2-2* from seedling leaf blades ($n = 4$; ***, $P < 0.001$). C, Easy-shattering phenotypes of *cad2* mutants ($n = 10$ or more; ***, $P < 0.001$). D to F, Longitudinal sections across the AZ after heading from the cv Dongjin wild type (D), *cad2-1* (E), and *cad2-2* (F). Sections were stained with Toluidine Blue. Arrows indicate AZ. Bars = 100 μm. G to I, Longitudinal sections across the AZ after heading from the cv Dongjin wild type (G), *cad2-1* (H), and *cad2-2* (I). Sections were observed under UV light. Arrows indicate AZ. Bars = 100 μm.

supported our conclusion that lignin deposition in the pedicle plays an important role in determining the degree of seed shattering.

The OSH15-SH5 TALE-HD Complex Directly Represses *CAD2*

To examine whether OSH15 interacts directly with *CAD2*, we performed chromatin immunoprecipitation (ChIP) assays with OSH15-Myc-overexpressing transgenic plants. Because plants that overexpress *OSH15* display a multiple-shoot phenotype and most (greater than 90%) do not grow to maturity (Nagasaki et al., 2001), we examined seedling roots. These assays showed that the promoter regions (P5 and P6) and the genic areas (P6, P7, and P8) of *CAD2* chromatin were enriched by Myc antibodies (Fig. 10, A and B).

We also generated transgenic rice plants expressing SH5-Myc fusion protein and used the IM regions of the second internode at the preheading stage for the assays. There, the promoter regions as well as the genic regions of *CAD2* chromatin were enriched by the antibodies (Fig. 10, A and D). As a control, we used the *Ehd1* chromatin region, which functions as a flowering regulator (Cho et al., 2016), and found that it was not changed in the transgenic plants that expressed Myc-tagged OSH15 and SH5 (Fig. 10, C and E). These results

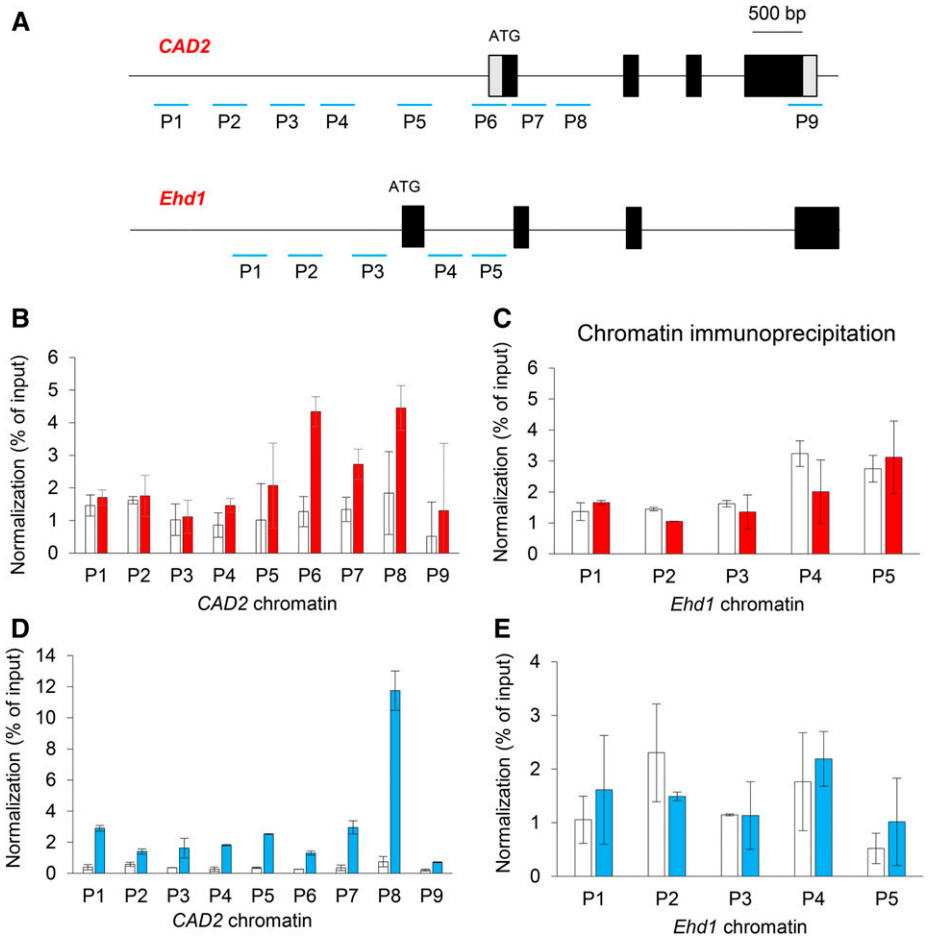

Figure 10. Assays of ChIP in *CAD2* chromatin regions with OSH15-Myc and SH5-Myc transgenic plants. A, Genomic structures of *CAD2* and *Ehd1*. Tested regions are numbered. B, Assay of OSH15 enrichment in *CAD2* chromatin regions. The experiment involved root samples taken from OSH15-Myc transgenic seedlings, and the percentage of input method was used for normalization. Transgenic plants expressing Myc alone were used as a negative control. C, Assay of OSH15 enrichment in *Ehd1* chromatin regions. D, Assay of SH5 enrichment in *CAD2* chromatin regions. The IM region of SH5-Myc transgenic plants was examined when the second internode was approximately 3 cm long. E, Assay of SH5 enrichment in *Ehd1* chromatin regions.

supported our theory that OSH15 and SH5 directly repress the expression of *CAD2*.

DISCUSSION

OSH15-qSH1 Dimer Functions for AZ Development

Heterodimers of a KNOX protein and a BELL protein play diverse biological functions (Mele et al., 2003; Smith and Hake, 2003; Rutjens et al., 2009; Khan et al., 2012). However, their roles in seed shattering have not been reported previously. In the SAM, the Arabidopsis BELL protein REPLUMLESS (RPL) interacts physically with the KNOX proteins SHOOTMERISTEMLESS, BP/KNAT1, and KNAT6 to regulate meristem development (Smith and Hake, 2003). RPL also controls replum development by repressing the preferential expression of the valve and valve margin genes for seed dehiscence (Marsch-Martínez et al., 2014).

The interaction between OSH15 and qSH1 suggests that they form a heterodimer that promotes AZ development. Mutation of *OSH15* causes an AZ defect in cv Dongjin where *SH5* expression is suppressed during AZ development as well as one in cv Kasalath where *SH5* is expressed in the AZ. This indicates that the control of such development by OSH15 is not dependent on SH5 (Fig. 11).

The AZ contains small, thin-walled cells with dense cytoplasm and no central vacuole (Sexton and Roberts, 1982). This set of cellular characteristics is reminiscent of meristematic tissues. Several genes involved in SAM maintenance and the initiation of axillary meristems are expressed in the AZ (Shi et al., 2011; Nakano et al., 2013; Wang et al., 2013). Therefore, it has been proposed that AZ cells have a meristematic identity. Because lignin deposition is a feature of irreversible cell differentiation, the prevention of expression for genes involved in lignin biosynthesis should be necessary for AZ formation (Yoon et al., 2014). However, the lignification of tissues contiguous to those that will experience cell separation appears to be required if abscission is to occur. That is the case for the lignification of the endothecium and the valve margin cells, which are essential to provide the mechanical force needed for anther dehiscence and pod shattering, respectively, in Arabidopsis (Steiner-Lange et al., 2003; Mitsuda and Ohme-Takagi, 2008).

The seed pods from Arabidopsis comprise three tissue types: two laterally positioned valves that protect

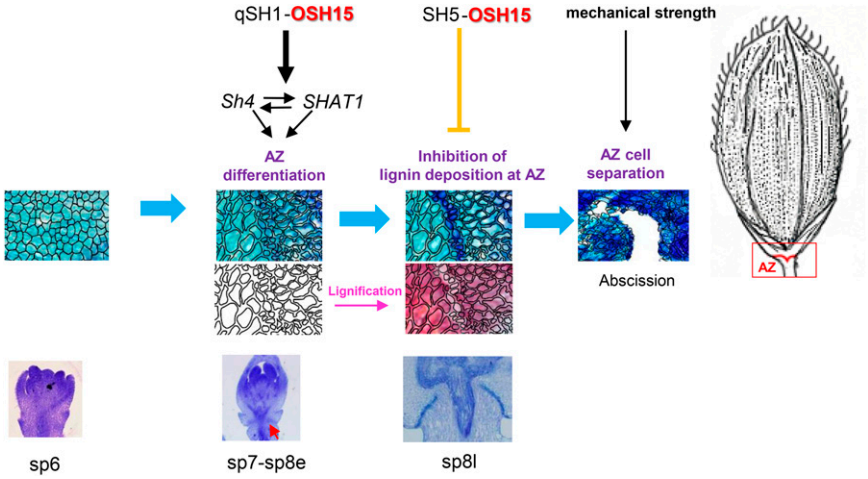

Figure 11. Model for seed shattering in rice.

seeds; the replum, a thin ridge of cells where the seeds are attached; and two valve margins that connect the replum and valve (Lewis et al., 2006). The valve margin consists of two types of cell layers: a lignified layer and a separation layer. At maturity, separation of this valve margin allows the fruit to open for seed dispersal (Lewis et al., 2006). Whereas the dehiscence zone in Arabidopsis is located in the valve margin, that AZ develops at the base of the pedicel in rice (Dong and Wang, 2015). In rice, *SH5* overexpression causes easy shattering by inhibiting lignin deposition at the AZ (Yoon et al., 2014). It is different from Arabidopsis pod dehiscence, which produces a spring-like tension within the pod valves that forces the silique to shatter from the weakest position, the separation layer (Dong and Wang, 2015).

The OSH15-SH5 Dimer Functions in Lignin Biosynthesis

When compared with the wild type, the suppression of *OSH15* expression caused more lignin to accumulate in the AZ. Similarly, the *osh15* mutant accumulated more lignin in the developing second internode. These observations indicated that one of the functions of *OSH15* is to inhibit lignin accumulation. We have reported previously that *SH5* also blocks lignin deposition in the grain pedicel region (Yoon et al., 2014). Because OSH15 interacts with SH5, this OSH15-SH5 complex appears to suppress lignin accumulation.

The expression of several lignin biosynthesis genes was increased in the *osh15* mutants. In contrast, lignin biosynthesis genes are suppressed in *SH5* overexpression plants (Yoon et al., 2014). These observations provide supporting evidence that the OSH15-SH5 complex inhibits the genes involved in lignin biosynthesis. We found that both OSH15 and SH5 bind to *CAD2* chromatin. Mutations on *CAD2* also caused easy shattering, further demonstrating that lignin plays an important role in that phenomenon. Our results are consistent with a previous report that overexpression of a KNOX gene in maize and tobacco (*Nicotiana tabacum*) reduces lignin concentrations by inhibiting at least two steps in that biosynthesis pathway (Townsley et al., 2013).

Internode Development Is Controlled by OSH15

Mutations in *OSH15* caused a repression of internode elongation. Similar dwarf phenotypes have been described for *bp* mutants from Arabidopsis (Sato et al., 1998, 1999; Mele et al., 2003). In the *bp* mutant, transcript levels of lignin biosynthesis genes are increased (Mele et al., 2003). KNOX genes are expressed preferentially in the indeterminate cells around the SAM and are necessary for its formation and maintenance (Hake et al., 2004; Tsuda et al., 2011). These observations suggest that KNOX proteins function in maintaining the SAM and repressing lignin deposition during its development.

We observed that *OSH15* was expressed universally in internode tissues. However, *SH5* is expressed preferentially in the IM (Yoon et al., 2015). Therefore, the OSH15-SH5 TALE-HD complex appears to repress lignin biosynthesis specifically in the IM during the process of internode development.

Both *OSH1* and *OSH15* are expressed during embryogenesis before the SAM develops (Sentoku et al., 1999). The *osh1* null mutants have a defect in that meristem. More than 90% of *osh1* mutants are seedling lethal, and only a low proportion of mutants reaches the six-leaf stage (Tsuda et al., 2011). In the *osh1 osh15* double mutant, embryo development failed completely, thereby implying that both *OSH1* and *OSH15* function in SAM formation (Tsuda et al., 2011). In contrast, *osh15* single mutants developed a normal SAM even though internode elongation was significantly retarded. These findings suggested that KNOX proteins have diverse functions when they interact with different BELL proteins.

MATERIALS AND METHODS

Plant Materials and Characterization of Mutant Phenotypes

The T-DNA tagging lines were generated in *japonica* rice (*Oryza sativa*) 'Dongjin' (Jeong et al., 2002; Yi and An, 2013). Panicles were harvested at the mature stage, and the degree of shattering was assessed after the BTS of the pedicels was measured with a digital force gauge (SHIMPO; http://www.shimpodrives.com/). Each BTS value represented an average of more than 15 samples from the uppermost part of the panicles (Ji et al., 2006).

RNA Isolation and qRT-PCR

Total RNA was isolated from leaf blade and internode samples with RNAiso Plus (TaKaRa). First-strand cDNA was synthesized with 2 μg of total RNA and Moloney murine leukemia virus reverse transcriptase (Promega; http://www.promega.com/) plus 10 ng of the oligo(dT) primer and 2.5 mM deoxyribonucleotide triphosphate. Synthesized cDNAs and SYBR Premix Ex Taq (TaKaRa) were used for real-time qRT-PCR on a Rotor-Gene Q system (Qiagen; http://www.qiagen.com/). Transcript levels were normalized with *OsUbi*, and the $\Delta\Delta$Ct method was applied to calculate levels of relative expression (Choi et al., 2014). All primers for quantitative real-time PCR are listed in Supplemental Table S1.

Vector Construction and Rice Transformation

For construction of the *OSH15* RNAi vector, a 265-bp 3′ UTR between –71 bp and +191 bp from the translation stop site was ligated into the pGA3426 binary vector with an ampicillin linker (Kim et al., 2009; Yoon et al., 2014). The *OSH15* promoter-GUS vector was made by inserting the 1.7-kb promoter region (between –1,707 and –55 bp) from the translation start site ATG of *OSH15* into the pGA3519 binary vector. All primers are presented in Supplemental Table S1. The constructs were transformed into *Agrobacterium tumefaciens* LBA4404 as described previously (An et al., 1988). Both RNAi and GUS-promoter transgenic plants were generated by a stable rice transformation method via *A. tumefaciens*-mediated cocultivation (Lee et al., 1999).

Histochemical Analysis and GUS Assay

Spikelet and internode samples were fixed in a formalin-acetic acid-alcohol solution and stored at 4°C. After dehydration through an ethanol series, the samples were incubated in a *tert*-butyl alcohol series and then completely infiltrated with paraffin. They were then placed in an embedding ring. Tissues were sectioned to 10 μm thickness with a microtome (model 2165; Leica Microsystems; http://www.leica-microsystems.com/) and then stained with either Toluidine Blue, which interacts mainly with nucleic acids, or phloroglucinol-HCl, which interacts with coniferaldehyde and sinapaldehyde end groups, to distinguish the lignified cell walls (Anderson et al., 2015). All samples were observed with a BX microscope (Olympus; http://www.olympus-global.com/en/). Lignin polymerization was examined by the UV imaging method (Mele et al., 2003). Briefly, samples were embedded in paraffin, sectioned to a 10-mm thickness, and cleared with xylene without any histochemical staining. They were observed with a BX61 microscope (Olympus) with UV light at 360 to 370 nm excitation and 420 to 460 nm emission.

For GUS assays, samples were incubated overnight at 37°C in a GUS solution containing 100 mM sodium phosphate (pH 7), 5 mM potassium ferricyanide, 5 mM potassium ferrocyanide, 0.5% (v/v) Triton X-100, 10 mM EDTA (pH 8), 0.1% (w/v) 5-bromo-4-chloro-3-indolyl-β-D-GlcA/cyclohexylammonium salt, 2% (v/v) dimethyl sulfoxide, and 5% (v/v) methanol (Kim et al., 2013). The stained samples were treated with Viskol clearing reagent (Phytosys; http://visikol.com/) and then observed for GUS activity with the BX microscope.

Co-IP Assay

To construct the Myc or HA fusion molecules, *SH5*, *qSH1*, and *OSH15* full-length cDNAs without the stop codons were inserted into pGA3817 with the 6× Myc coding region or into pGA3818 with the 3× HA. Primers for full-length amplifications are presented in Supplemental Table S1. These fusion molecules were transformed into protoplasts isolated from rice suspension cells, and Co-IP assays were performed as described previously (Choi et al., 2014; Cho et al., 2016). Briefly, fusion proteins were coimmunoprecipitated using the anti-HA mouse monoclonal antibodies (12CA5; Roche; http://www.roche.com) conjugated with A and G agarose beads (Millipore; http://www.emdmillipore.com). The immunoprecipitation buffer consisted of 75 mM NaCl, 50 mM Tris-HCl (pH 7.5), 5 mM EDTA, 1% Triton X-100, 1 mM DTT, 1 mM phenylmethanesulfonyl fluoride, 2 mM NaF, 20 μM MG132, and the proper amount of protease inhibitor cocktail (Roche). The eluted proteins were resolved by 10% SDS-PAGE and transferred to a polyvinylidene difluoride membrane (Millipore). Horseradish peroxidase-conjugated anti-Myc monoclonal antibody (2040; Cell Signaling) and anti-HA monoclonal antibody (2999; Cell Signaling) were used for protein detection. The ECL Prime western blotting detection reagent (RPN2232; GE Healthcare; http://www.gelifesciences.com) was used in LAS-4000 (GE Healthcare).

ChIP Analysis

ChIP was performed as described previously (Haring et al., 2007). Briefly, 2 g of fresh roots and internode samples was incubated in 3% formaldehyde. After nuclei isolation, chromatins were sheared to about 500 to 1,000 bp by sonication. Before preclearing, 1% of the sample was collected as an input. For immunoprecipitation, we used anti-Myc monoclonal antibodies (2276; Cell Signaling) as reported previously (Yang et al., 2013). Data were normalized according to the percentage of input method (Haring et al., 2007). Primers for this work are listed in Supplemental Table S2.

Supplemental Data

The following supplemental materials are available.

Supplemental Figure S1. Expression patterns of OSH15.

Supplemental Figure S2. Phylogenetic analysis and schematic diagram of TALE-HD members.

Supplemental Figure S3. Expression of shattering-related genes in *OSH15* RNAi lines.

Supplemental Figure S4. Analysis of *OSH15* cv Kasalath RNAi transgenic rice plants.

Supplemental Table S1. Primers used in this study.

Supplemental Table S2. Primers used in the ChIP assay.

ACKNOWLEDGMENTS

We thank Kyungsook An for handling the seed stock and Priscilla Licht for editing the English composition of the article.

Received February 27, 2017; accepted March 23, 2017; published March 28, 2017.

LITERATURE CITED

An G, Ebert PR, Mitra A, Ha SB (1988) Binary vectors. *In* SB Gelvin, RA Schilperoort, eds, Plant Molecular Biology Manual. Kluwer Academic Publishers, Dordrecht, The Netherlands, pp 1–19

Anderson NA, Tobimatsu Y, Ciesielski PN, Ximenes E, Ralph J, Donohoe BS, Ladisch M, Chapple C (2015) Manipulation of guaiacyl and syringyl monomer biosynthesis in an *Arabidopsis* cinnamyl alcohol dehydrogenase mutant results in atypical lignin biosynthesis and modified cell wall structure. Plant Cell **27:** 2195–2209

Chen H, Rosin FM, Prat S, Hannapel DJ (2003) Interacting transcription factors from the three-amino acid loop extension superclass regulate tuber formation. Plant Physiol **132:** 1391–1404

Cho LH, Yoon J, Pasriga R, An G (2016) Homodimerization of Ehd1 is required to induce flowering in rice. Plant Physiol **170:** 2159–2171

Choi SC, Lee S, Kim SR, Lee YS, Liu C, Cao X, An G (2014) Trithorax group protein *Oryza sativa* Trithorax1 controls flowering time in rice via interaction with *early heading date3*. Plant Physiol **164:** 1326–1337

Dong Y, Wang YZ (2015) Seed shattering: from models to crops. Front Plant Sci **6:** 476

Dong Y, Yang X, Liu J, Wang BH, Liu BL, Wang YZ (2014) Pod shattering resistance associated with domestication is mediated by a NAC gene in soybean. Nat Commun **5:** 3352

Estornell LH, Agustí J, Merelo P, Talón M, Tadeo FR (2013) Elucidating mechanisms underlying organ abscission. Plant Sci **199-200:** 48–60

Fuller DQ, Allaby R (2009) Seed dispersal and crop domestication: shattering, germination, and seasonality in evolution under cultivation. Annu Plant Rev **38:** 238–295

Hake S, Smith HMS, Holtan H, Magnani E, Mele G, Ramirez J (2004) The role of *knox* genes in plant development. Annu Rev Cell Dev Biol **20:** 125–151

Haring M, Offermann S, Danker T, Horst I, Peterhansel C, Stam M (2007) Chromatin immunoprecipitation: optimization, quantitative analysis and data normalization. Plant Methods **3:** 11

Hay A, Tsiantis M (2010) KNOX genes: versatile regulators of plant development and diversity. Development **137:** 3153–3165

Hirano K, Aya K, Kondo M, Okuno A, Morinaka Y, Matsuoka M (2012) *OsCAD2* is the major *CAD* gene responsible for monolignol biosynthesis in rice culm. Plant Cell Rep **31:** 91–101

Itoh J, Nonomura K, Ikeda K, Yamaki S, Inukai Y, Yamagishi H, Kitano H, Nagato Y (2005) Rice plant development: from zygote to spikelet. Plant Cell Physiol **46:** 23–47

Jeong DH, An S, Kang HG, Moon S, Han JJ, Park S, Lee HS, An K, An G (2002) T-DNA insertional mutagenesis for activation tagging in rice. Plant Physiol **130:** 1636–1644

Ji H, Kim SR, Kim YH, Kim H, Eun MY, Jin ID, Cha YS, Yun DW, Ahn BO, Lee MC, et al (2010) Inactivation of the CTD phosphatase-like gene *OsCPL1* enhances the development of the abscission layer and seed shattering in rice. Plant J **61:** 96–106

Ji HS, Chu SH, Jiang W, Cho YI, Hahn JH, Eun MY, McCouch SR, Koh HJ (2006) Characterization and mapping of a shattering mutant in rice that corresponds to a block of domestication genes. Genetics **173:** 995–1005

Kanrar S, Onguka O, Smith HM (2006) *Arabidopsis* inflorescence architecture requires the activities of KNOX-BELL homeodomain heterodimers. Planta **224:** 1163–1173

Khan M, Xu M, Murmu J, Tabb P, Liu Y, Storey K, McKim SM, Douglas CJ, Hepworth SR (2012) Antagonistic interaction of BLADE-ON-PETIOLE1 and 2 with BREVIPEDICELLUS and PENNYWISE regulates *Arabidopsis* inflorescence architecture. Plant Physiol **158:** 946–960

Kim SL, Choi M, Jung KH, An G (2013) Analysis of the early-flowering mechanisms and generation of T-DNA tagging lines in Kitaake, a model rice cultivar. J Exp Bot **64:** 4169–4182

Kim SR, Lee DY, Yang JI, Moon S, An G (2009) Cloning vectors for rice. J Plant Biol **52:** 73–78

Konishi S, Izawa T, Lin SY, Ebana K, Fukuta Y, Sasaki T, Yano M (2006) An SNP caused loss of seed shattering during rice domestication. Science **312:** 1392–1396

Lee S, Jeon JS, Jung KH, An G (1999) Binary vectors for efficient transformation of rice. J Plant Biol **42:** 310–316

Lewis MW, Leslie ME, Liljegren SJ (2006) Plant separation: 50 ways to leave your mother. Curr Opin Plant Biol **9:** 59–65

Li C, Zhou A, Sang T (2006) Rice domestication by reducing shattering. Science **311:** 1936–1939

Li X, Yang Y, Yao J, Chen G, Li X, Zhang Q, Wu C (2009) *FLEXIBLE CULM 1* encoding a cinnamyl-alcohol dehydrogenase controls culm mechanical strength in rice. Plant Mol Biol **69:** 685–697

Luo L, Li W, Miura K, Ashikari M, Kyozuka J (2012) Control of tiller growth of rice by *OsSPL14* and strigolactones, which work in two independent pathways. Plant Cell Physiol **53:** 1793–1801

Marsch-Martínez N, Zúñiga-Mayo VM, Herrera-Ubaldo H, Ouwerkerk PB, Pablo-Villa J, Lozano-Sotomayor P, Greco R, Ballester P, Balanzá V, Kuijt SJ, et al (2014) The NTT transcription factor promotes replum development in Arabidopsis fruits. Plant J **80:** 69–81

Mele G, Ori N, Sato Y, Hake S (2003) The knotted1-like homeobox gene *BREVIPEDICELLUS* regulates cell differentiation by modulating metabolic pathways. Genes Dev **17:** 2088–2093

Mitsuda N, Ohme-Takagi M (2008) NAC transcription factors NST1 and NST3 regulate pod shattering in a partially redundant manner by promoting secondary wall formation after the establishment of tissue identity. Plant J **56:** 768–778

Müller J, Wang Y, Franzen R, Santi L, Salamini F, Rohde W (2001) In vitro interactions between barley TALE homeodomain proteins suggest a role for protein-protein associations in the regulation of Knox gene function. Plant J **27:** 13–23

Nagasaki H, Sakamoto T, Sato Y, Matsuoka M (2001) Functional analysis of the conserved domains of a rice KNOX homeodomain protein, OSH15. Plant Cell **13:** 2085–2098

Nakano T, Fujisawa M, Shima Y, Ito Y (2013) Expression profiling of tomato pre-abscission pedicels provides insights into abscission zone properties including competence to respond to abscission signals. BMC Plant Biol **13:** 40

Rutjens B, Bao D, van Eck-Stouten E, Brand M, Smeekens S, Proveniers M (2009) Shoot apical meristem function in *Arabidopsis* requires the combined activities of three BEL1-like homeodomain proteins. Plant J **58:** 641–654

Sato Y, Hong SK, Tagiri A, Kitano H, Yamamoto N, Nagato Y, Matsuoka M (1996) A rice homeobox gene, *OSH1*, is expressed before organ differentiation in a specific region during early embryogenesis. Proc Natl Acad Sci USA **93:** 8117–8122

Sato Y, Sentoku N, Miura Y, Hirochika H, Kitano H, Matsuoka M (1999) Loss-of-function mutations in the rice homeobox gene *OSH15* affect the architecture of internodes resulting in dwarf plants. EMBO J **18:** 992–1002

Sato Y, Sentoku N, Nagato Y, Matsuoka M (1998) Isolation and characterization of a rice homebox gene, OSH15. Plant Mol Biol **38:** 983–998

Sentoku N, Sato Y, Kurata N, Ito Y, Kitano H, Matsuoka M (1999) Regional expression of the rice *KN1*-type homeobox gene family during embryo, shoot, and flower development. Plant Cell **11:** 1651–1664

Sexton R, Roberts JA (1982) Cell biology of abscission. Annu Rev Plant Physiol **33:** 133–162

Shi CL, Stenvik GE, Vie AK, Bones AM, Pautot V, Proveniers M, Aalen RB, Butenko MA (2011) *Arabidopsis* class I KNOTTED-like homeobox proteins act downstream in the IDA-HAE/HSL2 floral abscission signaling pathway. Plant Cell **23:** 2553–2567

Smith HM, Boschke I, Hake S (2002) Selective interaction of plant homeodomain proteins mediates high DNA-binding affinity. Proc Natl Acad Sci USA **99:** 9579–9584

Smith HM, Hake S (2003) The interaction of two homeobox genes, *BREVIPEDICELLUS* and *PENNYWISE*, regulates internode patterning in the Arabidopsis inflorescence. Plant Cell **15:** 1717–1727

Steiner-Lange S, Unte US, Eckstein L, Yang C, Wilson ZA, Schmelzer E, Dekker K, Saedler H (2003) Disruption of Arabidopsis thaliana MYB26 results in male sterility due to non-dehiscent anthers. Plant J **34:** 519–528

Townsley BT, Sinha NR, Kang J (2013) KNOX1 genes regulate lignin deposition and composition in monocots and dicots. Front Plant Sci **4:** 121

Tsuda K, Ito Y, Sato Y, Kurata N (2011) Positive autoregulation of a *KNOX* gene is essential for shoot apical meristem maintenance in rice. Plant Cell **23:** 4368–4381

Venglat SP, Dumonceaux T, Rozwadowski K, Parnell L, Babic V, Keller W, Martienssen R, Selvaraj G, Datla R (2002) The homeobox gene *BREVIPEDICELLUS* is a key regulator of inflorescence architecture in *Arabidopsis*. Proc Natl Acad Sci USA **99:** 4730–4735

Wang X, Liu D, Li A, Sun X, Zhang R, Wu L, Liang Y, Mao L (2013) Transcriptome analysis of tomato flower pedicel tissues reveals abscission zone-specific modulation of key meristem activity genes. PLoS ONE **8:** e55238

Yang J, Lee S, Hang R, Kim SR, Lee YS, Cao X, Amasino R, An G (2013) OsVIL2 functions with PRC2 to induce flowering by repressing *OsLFL1* in rice. Plant J **73:** 566–578

Yi J, An G (2013) Utilization of T-DNA tagging lines in rice. J Plant Biol **56:** 85–90

Yoon J, Cho LH, Kim SL, Choi H, Koh HJ, An G (2014) The BEL1-type homeobox gene *SH5* induces seed shattering by enhancing abscission-zone development and inhibiting lignin biosynthesis. Plant J **79:** 717–728

Yoon J, Choi H, An G (2015) Roles of lignin biosynthesis and regulatory genes in plant development. J Integr Plant Biol **57:** 902–912

Zhou Y, Lu D, Li C, Luo J, Zhu BF, Zhu J, Shangguan Y, Wang Z, Sang T, Zhou B, et al (2012) Genetic control of seed shattering in rice by the APETALA2 transcription factor *shattering abortion1*. Plant Cell **24:** 1034–1048